A. Dlouhý
Slip processes in non-uniformly distributed dislocation structures
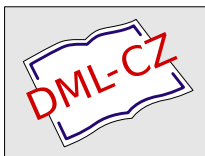
Slip Processes in Non-Uniformly Distributed Dislocation Structures

A. DLOUHÝ*)

Czechoslovakia

Introduction

The dislocation structures with non-homogeneously distributed dislocation density are frequently observed in the course of plastic deformation of crystalline materials [1, 2]. This experimental phenomenon has been recently involved into the models [3, 4] describing stress distribution in dislocation structures created during the plastic deformation of metals. In spite of the fact that these models were successfully applied to the explanation of some experimental results [5], there still remain problems with kinetic aspects of the deformation process [6]. Considering this set of models [3, 4] it is not easy to elucidate, for example, the stress dependence of the strain rate obtained from creep experiments [7].

Another group of problems. closely connected with the kinetic properties and still open to discussion, is associated with the theory and measurement of the internal stress acting on moving dislocations [8].

We have tried to find a metodical tool capable to solve some of the mentioned problems. The computer treatment of the model proposed below is probably one of the possible ways to build up such a tool. In the present paper, some preliminary results obtained in computer experiments are discussed.

Model

It is assumed that slip processes occur on parallel slip planes (marked Σ_i in Fig. 1.) due to a movement of long strainght dislocations parallel to the y-axis (movement on the slip system Σ). The spacing between neighbouring slip planes is z_0. The non--uniformly distributed dislocation forest forms structural obstacles to the dislocation motion in the slip system Σ. The dislocation forest has different densities in different regions of the slip plane. Fig. 2. While in the *soft regions S* low dislocation forest density ϱ_S is presented, there is a rather high obstacle density ϱ_H in the *hard*

*) Czechoslovak Academy of Sciences, Institute of Physical Metallurgy, 616 62 Brno, Czechoslovakia.

regions H. The size of one dislocation cell, x_0, is composed of space dimension of the *S*-region. x_S, and of x_H which is the *H*-region size.

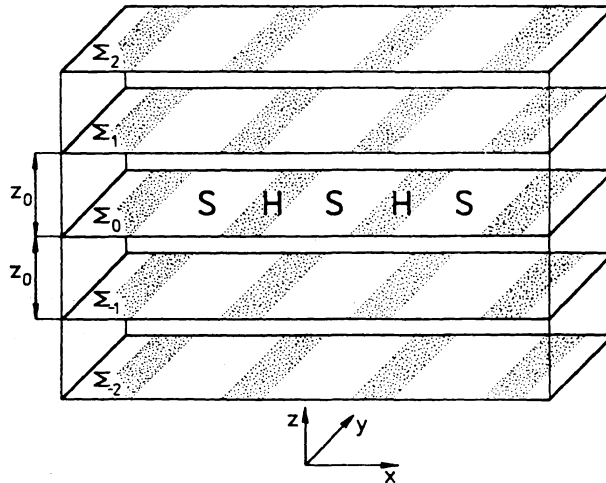The described distribution of the forest dislocation density gives rise to correspond-

Fig. 1. The set of z_0 spaced parallel slip planes Σ_i within a crystal. Hard *H* and soft *S* regions are more (*H*) or less (*S*) populated by the dislocation forest.
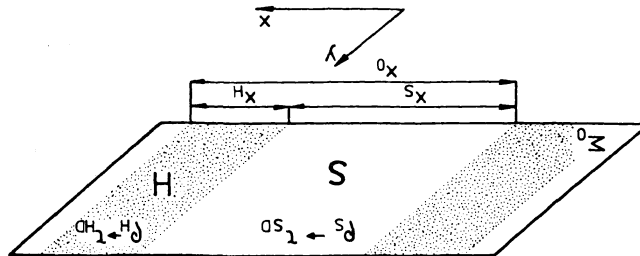

Fig. 2. Soft and hard region sizes are x_S and x_H respectively, x_0 is the size of one dislocation cell. The dislocation forest densities ϱ_S and ϱ_H and corresponding slip resistances τ_{SD} and τ_{HD} are also indicated inside every region.

ing distribution of the slip resistances τ_{RD}, τ_{RD} are defined as:

$$(1) \qquad\qquad \tau_{RD} = \alpha\mu b \sqrt{\varrho_R}$$

where *R* is *S* or *H*, $\alpha \approx 1$ is a number constant, μ is the shear modulus and *b* is the magnitude of the Burgers vector, In the case of solid solution alloys the *total local slip resistance*, τ_R, includes both τ_{RD} and τ_A, where τ_A arises due to presence of alloying elements. Under some assumptions specified in [9], the following equation holds:

$$(2) \qquad\qquad \tau_R = \tau_{RD} + \tau_A .$$

54

The long-range internal stress field acting on a dislocation slipping on a Σ_i-plane originates from mutual interaction between this dislocation and the other ones moving on the slip system Σ. As the dislocation forest cannot cause long-range internal stress field in the slip system Σ, it is possible to describe the *total long-range internal stress fileld acting on the j-th mobile dislocation* as:

$$(3) \qquad \tau_{iD}^j = \sum_{k \neq j} \delta_{jk} \frac{\mu b}{R_{jk}}$$

where the indes k scans the group of mobile dislocations. δ_{jk} are the interaction coefficients, and R_{jk} is the distance between the j-th and k-th dislocation.

Let the origin of the x-axis correspond to the centre of a S-region (Fig. 2). The creation of mobile dislocations takes place at Frank — Read type dislocation sources situated at the points $x_S = p x_0 / 2$, where p is an integer. A new dislocation loop is created when the externally applied shear stress, τ_a, plus *internal stress* (eq. 3) at the points $x_S \pm x_{SOURCE}$ exceeds *slip resistance* τ_R (eq. 2) in the region. The distance x_{SOURCE} is then given as:

$$(4) \qquad x_{SOURCE} = \frac{\mu b}{2 \tau_{RD}}$$

where τ_{RD} are described by eq. 1.

The j-th dislocation is moving when, at its position, the following condition holds:

$$(5) \qquad |\tau_a + \tau_{iD}^j| > \tau_R$$

in this case, the j-th dislocation can slip over the distance:

$$(6) \qquad \Delta x_D^j = \frac{\tau_a + \tau_{iD}^j \pm \tau_R}{\beta} \Delta t$$

here β is the coefficient of viscous motion and Δt is the time increment. If the stress $\tau_a + \tau_{iD}^j$ is positive, then a negative sign in eq. 6 is applied.

In the model described, a simple recovery proccess has been proposed. The dislocations with the opposite sign mutually annihilate each other if their distance in plane Σ_i is less or equal to x_A, where:

$$(7) \qquad x_A = \delta_A \frac{\mu b}{\tau_R}$$

and constant δ_A depends on dislocation character.

Results and discussion

To maintain a bond between computer results and results of real deformation experiments, experimentally obtained values are used as an input set of structural parameters. For plastic deformation of Cu-Zn alloys following parameters were found [10, 11]: $\varrho_S \approx 4 \times 10^{13}$ m^{-2}, $\varrho_H \approx 1.7 \times 10^{14}$ m^{-2}, $x_S/x_0 \approx 0.7$, $x_0 \approx 2$ μm,

$z_0 \approx 3$ μm and $\tau_A \approx 10$ MPa. Creep processes were simulated so that this obstacle structure was subjected to the constant level of the applied stress, τ_a, in all computation runs. However, in *different* runs *different levels of the* τ_a were applied.

In every computation run, steady state stage of creep was reached. In this stage, the rate of slip deformation did not show any substantial changes during a large time period. This fact gave us the posibility to characterize the steady state stage by *steady state slip rate* $\dot{\gamma}_S$:

$$(8) \qquad\qquad \dot{\gamma}_S = \frac{b}{z_0 T_S}$$

where T_S is the time interval between two annihilation events. The dependence of the $\dot{\gamma}_S$ on τ_a is shown in Fig. 3. Below the threshold stress $\tau_{a0} = 108.3$ MPa, "global"
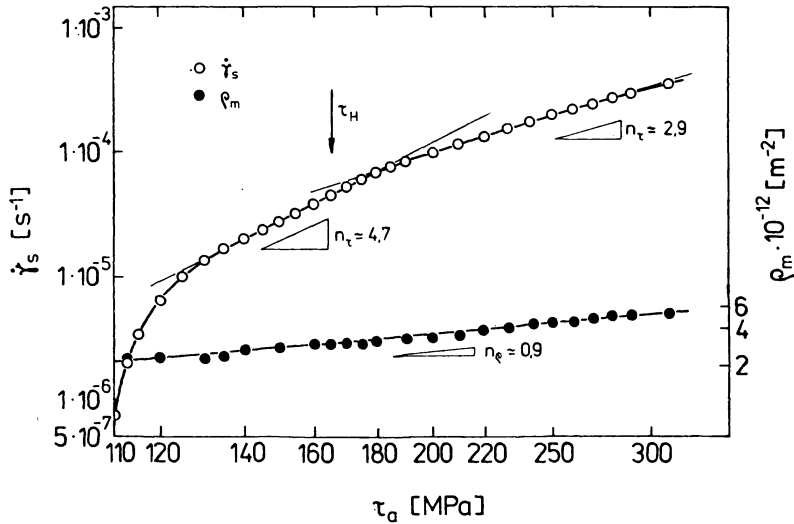
Fig. 3. Steady state slip rate $\dot{\gamma}_S$ and mobile dislocation density ϱ_m as functions of applied stress τ_a. The initial set of structure parameters was taken from Ref. [10, 11]. τ_H is the stress level necessary for activation of dislocation sources in hard regions.

slip deformation cannot occur and $\dot{\gamma}_S = 0$. This value of the threshold stress is in satisfactory agreement with that proposed for the given set of structural parameters using Mughrabi's [3] model $\left(\tau_{a0}^{MUGHRABI} = 108.4 \text{ MPa}\right)$. Above stress τ_{a0}. the deformation rate $\dot{\gamma}_S$ increases with increasing τ_a. In higher applied stress range, the dependence has the power law form with stress exponent n_τ changing from the value close to 5 to the value of about 3. It is also possible to describe the relationship between mobile dislocation density ϱ_m and applied streess τ_a by means of the power law dependence in the investigated stress range. In this case, stress exponent n_ϱ is close to 1.

It should be pointed out that the dependence of the slip rate $\dot{\gamma}_S$ on the applied shear stress τ_a does not correspond to the dependence of the steady state creep rate $\dot{\varepsilon}_S$ on the applied stress σ investigated in real creep experiments, one of the reasons is that, in this study, initial structure of the dislocation forest is the same for all applied stress levels and it is not allowed to change this structure during deformation to the steady state.

The internal stress is an important part of the driving force governing the dislocation motion. With respect to the internal stress definition (eq. 3) and to the equation 6, which controls dislocation velocity in this model, it is necessary to calculate τ_{iDj} many times during the course of dislocation motion. The calculation of the internal stress at any current dislocation position gives us the possibility to construct the *path dependence* $\tau_{iDj}(x_{Dj})$, it means, the position dependence of the long-range internal stress which the dislocation really feels at every point of its path. It is convenient to note again, that the internal stress and its path dependence arise only from mutual long-rage interaction among mobile dislocations and does not include any other stress components in this study.

The internal stress path dependence are shown in Figs. 4a) – d). These dependences were taken at the steady state deformation stage and the upper j-indexes were omitted in these figures. At the upper part of the figures, the dashed line represents the applied stress level τ_a; point $X1$ (soft region) and point $X2$ (hard region) indicate positions at which, being created, new parts of dislocation loops appears; annihilation events take place at the point $X3$. Dotted curves show the internal stress τ_{iD} path dependence while mean internal stress $\bar{\tau}_{iD}$ is drawn by the full line. As an example it is possible to give the definition of the mean internal stress in the soft region:

$$(9) \qquad \bar{\tau}_{iD}(x_D) = \frac{1}{x_D} \int_{X1}^{x_D} \tau_{iD}(x) \, dx .$$

A similar definition is valid in the hard region, too. The structure of the mobile dislocation group is demonstrated in the lower part of the figures. Point $XS/2$ shows boundary between the soft and the adjacent hard region.

It can be seen (Fig. 4a) that, at the lower applied stress limit, the path dependences closely resemble internal stress distribution proposed by Mughrabi [3]. There is also quantitative agreement between Mugrhabi's and our model, for example, at $\tau_a = 110$ MPa, we find $\tau_{iD} = -23$ MPa within the soft, and $\tau_{iD} = 59$ MPa within the hard region, while Mughrabi's approach gives -24.4 MPa and 57 MPa, respectively. The situation is slightly different when applied stress is higher. In this case, the internal stress has positive value in the hard region as well as on the appreciable part of the slip plane which is sparsely populated by the dislocation forest (Fig. 4c).

If we use the definition of soft and hard zones reflecting upon the internal stress distribution, then the soft zone is a part of the slip plane with the negative (backward) internal stress while the positive (forward) internal stress operates within the hard
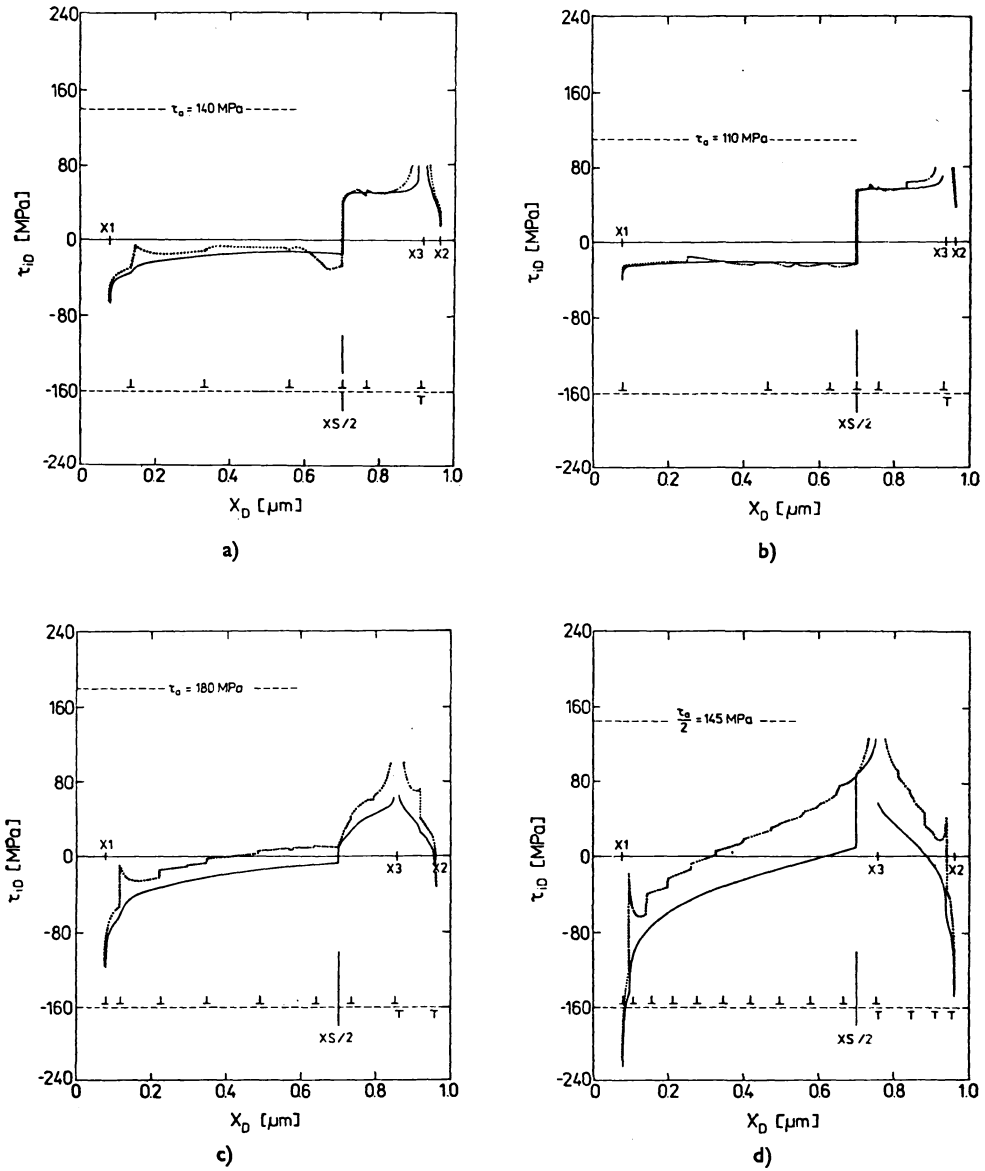
Fig. 4. Internal stress (dotted corve) and mean internal stress (full curve) path dependences for different levels of applied stress: a) $\tau_a = 110$ MPa, b) $\tau_a = 140$ MPa, c) $\tau_a = 180$ MPa and d) $\tau_a = 290$ MPa. The symmetry of the model allows to study these dependence in one half of soft region $x_D \in (0; \; XS/2)$ and in one adjoining half of hard region $x_D \in (XS/2; \; 1)$. Dislocations appear in points $X1$ and $X2$, annihilation point is indicated by $X3$. Configurations of the mobile dislocation group are shown in the lower part of figures just at the instant when two dislocations annihilate.

zone. Taking into consideration this "stress definition" it is evident from Figs. 4c and 4a that both soft and hard zone sizes are dependent on the level of the applied stress in spite of the fact that spacings x_S and x_H between regions with high and low dislocation forest densities and the forest densities themselves remain unchanged. At the highest applied stress examined (Fig. 4d) distinct internal stress differences observed at the lower applied stress range are completely removed. In this context it is also interesting to note that rather evident change in the stress exponent n_τ from 5 to 3 (Fig. 3) occurs in the same applied stress range, where sizes of the soft and hard zones begin to be dependent on the applied stress. This change takes place for the applied stress slightly above the stress τ_H (Fig. 3); τ_H being the stress level necessary for the activation of dislocation sources within hard regions.

Two severe oversimplifications are involved in the presented model. The first one is that no kind of the strain hardening is allowed during the course of plastic deformation with the exception of internal stress growth connected with the creation of the mobile dislocation group. The second oversimplification is based on eq. 6 because, in reality, thermally activated processes play an important role during the dislocation motion and the viscous mode of motion does not occur in most cases. Further work is being continued in order to study the influence which can be imposed on the presented results by relaxing these unrealistic assumptions.

Conclusions

In the present investigation, a simple model of dislocation motion through a non-uniformly distributed dislocation forest has been formulated and numerically solved. From these computer creep experiments following conclusions can be drawn:

1) Depending on the initial dislocation forest structure there is the applied stress threshold τ_{a0} below which „global" slip cannot occur.

2) Above τ_{a0} it is possible to reach the steady state deformation stage and to characterize this stage by the steady state slip rate $\dot{\gamma}_S$.

3) In a certain range of applied stresses, the dependence of the slip rate $\dot{\gamma}_S$ on the applied stress τ_a can be approximated by the power law with stress exponent n_τ changing from the value close to 5 to the value close to 3.

4) The change of the stress exponent n_τ takes place at the applied stress range where internal stress path dependences start to vary qualitatively.

5) At the low applied stress limit, the internal stress path dependences are in satisfactory agreement with the internal stress distribution proposed by Mughrabi [3]. The same statement is also valid for the threshold stress τ_{a0}.

6) The sizes of both the soft and hard regions are dependent on the applied stress level in the higher applied stress range.

References

[1] HANSEN, N. et al., Mater. Sci. Eng. 81, 1986, 141.
[2] MARTIN, J. L. et al., Mater. Sci. Eng. 81, 1986, 337.
[3] MUGHRABI, H., Acta Metall. 31, 1983, 1367.
[4] MUGHRABl, H., Mater. Sci. Eng. 85, 1987, 15.
[5] MUGHRABI, H. et al., Z. Metalkde. 77, 1986, 571.
[6] NABARRO, F. R. N., Acta Metall. 38, 1990, 637.
[7] BIBERGER, M. et al., Scripta Metall. 23, 1989, 1419.
[8] ČADEK, J., Mater. Sci. Eng. 94, 1987, 79.
[9] KOCKS, U. F. et al., Progr. Mater. Sci. 19, 1975, 160.
[10] PAHUTOVÁ, M. et al., Metallic Materials 27, 1989, 415.
[11] NEUHÄUSER, H., Acta Metall. 23, 1975, 455.